Growth Mechanism and Some Properties of $Cd_{1-x}Mn_x$ Se Semimagnetic Semiconductor Thin Films

V. S. KARANDE, S. H. MANE, V. B. PUJARI and L. P. DESHMUKH*

Department of Physics, Shivaji University Centre for Post Graduate Studies,
Solapur-Pune Road, Kegaon, Solapur 413002, MS., INDIA
e-mail: vskvikram@yahoo.co.in

Abstract

(Cd, Mn) Se dilute semiconductor or semimagnetic semiconductors have recently became the focus of intense research due to their interesting combination of magnetic and semiconducting properties, and are employed in a variety of devices including solar cells, gas sensors etc. A series of thin films of this material, $Cd_{1-x}Mn_xSe$ ($0 \leq x \leq 0.5$), were therefore synthesized onto precleaned amorphous glass substrates using a solution growth technique. The sources of cadmium (Cd^{2+}) and manganese (Mn^{2+}) were aqueous solutions of cadmium sulphate and manganese sulphate, and selenium (Se^{2-}) was extracted from a reflux of sodium selenosulphite. The different deposition parameters such as temperature, time of deposition, speed of mechanical churning, pH of the reaction mixture etc were optimized to yield good quality deposits. The as-grown samples were thin, relatively uniform, smooth and tightly adherent to the substrate support. The colour of the deposits changed from deep red-orange to yellowish-orange as the composition parameter, x, was varied from 0 to 0.5. The terminal layer thickness decreased with increasing value of, x. The optical energy gap decreased from 1.84 eV to 1.34 eV for the chang e of x from 0 to 0.5. The coefficient of optical absorption α is of the order of 10^4- 10^5 cm^{-1} and the type of transition (m $\cong$ 0.5) is of the band-to-band direct type. The dc electrical conductivities were measured at room temperature and in the temperature range 300 K - 500 K. It was observed that the room temperature electrical conductivity increased with the composition parameter x up to 0.1, gradually decreasing thereafter. The thermo power measurements showed n-type conduction in these films.

Key Words: Dilute semiconductor, reflux.

1.   Introduction

Magneto-optic semiconductors are known for their peculiar properties arising out of the exchange interaction between the mobile spins of the conduction electrons and localized spins of the incorporated magnetic elements [1-3]. It is, therefore, an interesting area of research in basic physics, with the task to learn how the magnetooptical phenomenon changes material properties in low dimensional nanostructures. In these structures, an electron wave function is transformed due to the quantum confinement effect, which in turn effects the exchange interaction between the conduction electrons and the localized magnetic moments [4, 5]. In addition, magnetic properties due to interaction between the localized moments should also be affected

*Corresponding author

due to a finite volume. Therefore, dimension and size of the magneto-optic system are of great technological importance as these parameters control the magneto-optic properties.

This is an attempt to synthesize a $Cd_{1-x}Mn_xSe$ magneto-optic system in its thin film form and to study its kinetics of film formation and a few of the physical properties.

2. Experimental Details

A series of $Cd_{1-x}Mn_xSe$ thin films of various x values ($0 \leq x \leq 0.5$) were obtained onto optically flat and thoroughly cleaned glass substrates by a solution growth technique [6 - 8]. For deposition, solutions of cadmium sulphate (1 M), manganese sulphate (1 M) and sodium selenosulphite (1 M, refluxed) in stoichiometric proportion were mixed as the sources for Cd^{2+}, Mn^{2+} and Se^{2-}, respectively. Aqua ammonia (NH_3) was added into the reaction container as a complexing agent and to adjust pH of the reaction mixture. The film deposition stoichiometry was maintained by adjusting atomic weights of the elements in solution for each of the compositions. Well-cleaned glass substrates were mounted on a bakelite substrate holder and the holder was kept rotating in a reaction mixture by means of a constant speed gear motor. This provides a continuous and uniform mechanical churning of the reaction mixture. To obtain good quality samples; the deposition time, temperature, pH and speed of the substrate rotation were optimized using a method described in [6].
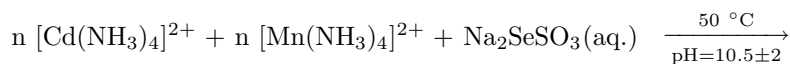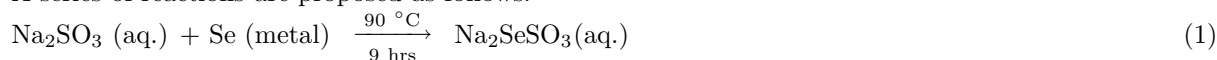
The terminal layer thicknesses of these as-deposited samples were measured using an interference technique. The film composition was checked by an energy dispersive spectroscopy technique. An X-ray diffraction method was used to determine the crystal structure of the samples. The range of scanning angles was from 20° to 80°. A Hitachi-330, spectrophotometer, was used to record the optical absorbance of the samples over the wavelength spectrum 400-1000 nm wavelength range. The optical gap E_g, absorption coefficient α and mode of transitions were then determined from these studies. The films were then characterized through the electrical conductivity and thermoelectric power measurement techniques measured over the temperature ranges 300 - 600 K and 300 - 450 K, respectively. A two-point probe contact method was used for these studies. Contacts at the ends of the films were constructed with silver paint. The activation energies, carrier concentration, mobility and intergrain barrier potentials were determined from these studies and the possible modes of conduction mechanism have been discussed.

3. Results and Discussion

3.1. Reaction mechanism, growth kinetics and physical observations

Co-deposition of Cd^{2+}, Mn^{2+} and Se^{2-} ions to form $Cd_{1-x}Mn_xSe$ thin film structures was carried out in an aqueous alkaline medium (pH $=10.5 \pm 0.2$) and with x in the range $0 \leq x \leq 0.5$. The deposition was initiated on the glass substrates in a reaction container consisting of a complex formed by salt solutions of cadmium, manganese, selenium and aqueous ammonia.

A series of reactions are proposed as follows:

$$Na_2SO_3 \text{ (aq.)} + Se \text{ (metal)} \xrightarrow[\text{9 hrs}]{90 \text{ °C}} Na_2SeSO_3\text{(aq.)} \tag{1}$$

$$CdSO_4 + 4NH_3 \longrightarrow [Cd(NH_3)_4]^{2+} \tag{2}$$

$$MnSO_4 + 4NH_3 \longrightarrow [Mn(NH_3)_4]^{2+} \tag{3}$$

$$n\,[Cd(NH_3)_4]^{2+} + n\,[Mn(NH_3)_4]^{2+} + Na_2SeSO_3\text{(aq.)} \xrightarrow[\text{pH}=10.5\pm2]{50 \text{ °C}}$$

$$Cd_{1-x}Mn_xSe \text{ (thin solid film)} + Na_2SO_4 + 8NH_3 \uparrow \qquad (4)$$

At room temperature and a few degrees above no film formation was observed, the reason being that, at such low temperatures, almost all the ions are in a complex-bound state [6-8]. The temperature of the reaction container was therefore varied from 30 °C to 70 °C, at which temperature, film formed and terminal layer thickness was measured. It was observed that the layer thickness increased almost linearly with increasing deposition temperature, to around 50 °C, but then decreased at higher deposition temperatures. Deposition thickness as a function of temperature is shown in Figure 1a. At temperatures up to 50 °C, thermal energy is sufficient to release ions from complex state thus enhancing layer thickness. Above this deposition temperature, the rate of reaction shifts towards precipitation rather than film formation; this is indicated by the presence of precipitate in the reaction container. As a result layer thickness decreased. The duration of the film growth was also studied. For this, the film deposition was prolonged up to three hours. The layer thickness was measured every half an hour and is plotted against time as shown in Figure 1b. It is seen that film growth is time-dependent and is initially quasilinear, then saturates. These observations have been understood from the fact that the volumetric ion concentration to surface substrate ratio decreases as time passes and finally results in a terminal layer thickness where this ratio is practically zero. The film growth was also examined for other crucial parameters, namely, speed of the substrate rotation and pH of the reaction mixture. A moderate speed of the substrate rotation (70 $\pm$ 2 rpm) was selected to obtain a sufficient layer thickness. The pH dependence of the film growth suggests that the films are porous, non-reflecting, flaky or powdery and adhered weakly to the substrate support for low values of the pH (7.5 to 9.5). On the other hand, at high deposition pH values (9.5 to 11), relatively uniform, nonporous, reflecting and tight adherent deposits are obtained. A pH value of 10.5 $\pm$ 0.2 was therefore selected and kept constant through out the deposition. Figure 1c shows a sketch of the average pH value versus the film layer thickness.

The as-grown CdSe samples are deep orange red in colour whereas the colour of the other compositions changed gradually to yellowish orange as x increased from 0 to 0.5. The change in color with the increased composition parameter x is an indication of substitution of Mn^{2+} in the host CdSe lattice. The terminal layer thickness was determined and is found to decrease as the composition parameter x increased. This is shown in Figure 1d.
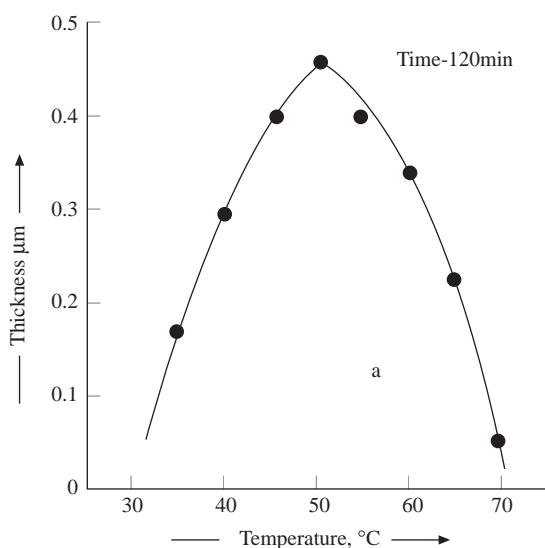

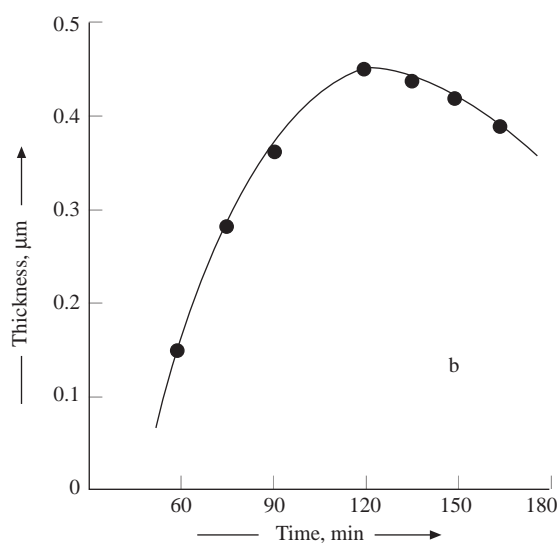**Figure 1a.** The terminal thickness versus deposition temperature at 120 minutes.

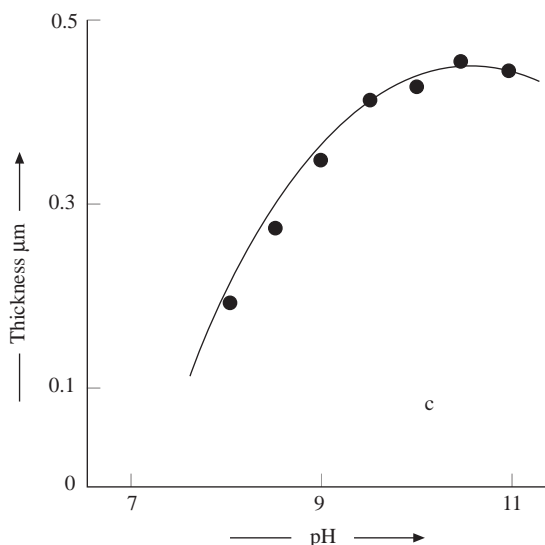**Figure 1b.** The terminal thickness versus deposition time at 50 °C.

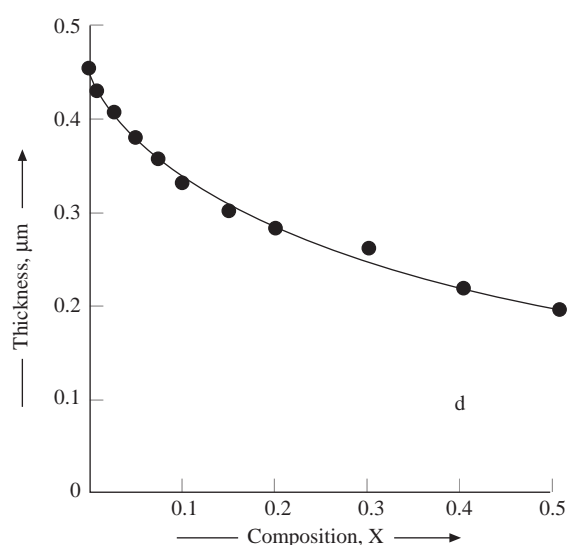**Figure 1c.** The terminal thickness versus pH for the above conditions.

Figure 1d. Variation of thickness with composition parameter, x.

3.2. Film composition studies

The film constituents (Cd^{2+}, Mn^{2+} and Se^{2-}) were determined quantitatively by an energy dispersive spectroscopy technique. As-grown CdSe is slightly Cd^{2+} rich and addition of Mn^{2+} in CdSe substitutes Cd^{2+}, whereas Se^{2-} content is practically constant. The contents of Cd^{2+}, Mn^{2+} and Se^{2-} for various film structures are shown in Table. It appears from the table that content of Cd^{2+} decreased with increasing Mn^{2+} content in the sample.

Table. Compositional analysis of $Cd_{1-x}Mn_xSe$ thin films.

Composition (x)	Cd content wt%	Mn content wt%	Se content wt%
0.00	55.45	-	44.55
0.01	53.61	-	44.81
0.025	52.94	0.91	46.15
0.075	52.19	1.37	46.44
0.1	56.17	1.81	42.0
0.15	52.19	3.98	43.83
0.3	50.77	4.14	45.09

The X-ray diffraction analysis of the samples was carried out over the 2θ range $20° \leq 2\theta \leq 80°$. The samples are hexagonal dominant polycrystals of the $Cd_{1-x}Mn_xSe$ type and are oriented along (100) direction. Upto $x = 0.1$, addition of Mn^{2+} in the CdSe lattice shifts the peak position towards the lower 2θ side and above $x = 0.1$ towards the higher 2θ side.

3.3. Optical properties

To obtain information on the optical characteristics of these materials, studies were conducted on these composite structures, to determine optical constants such as the absorption coefficient α, optical gap E_g and nature of the transitions. For all compositions, the absorption coefficient is of the order of 10^4 to 10^5 cm^{-1} and the absorption edges were determined by extrapolating the steep portion of the, α vs $h\nu$ plots

on the energy axis. The optical gaps were then determined by plotting $(\alpha h\nu)^2$ vs $h\nu$, as shown in Figure 2. It is seen that pure CdSe exhibits an optical gap equal to 1.84 eV, but decreases down to 1.34 eV as the Mn^{2+} concentration in the CdSe lattice increases to $x = 0.5$. Figure 3 shows variation of the optical gap with the composition x. It appears that the variation is almost linear and continuous. Figure 2 also show straight-line segments showing direct-type of transitions involved in these samples. These transitions were also supported by evaluation of the transition index m from variation of ln $(\alpha h\nu)$ vs ln $(h\nu$-$E_g)$ as shown in Figure 4 [8, 9].
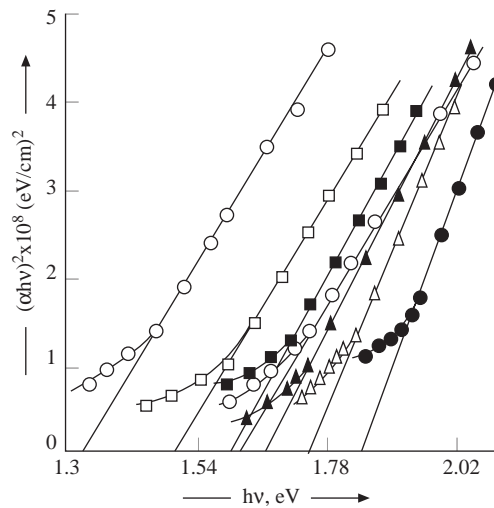

Figure 2. Plot of $(\alpha h\nu)^2$ versus $h\nu$ for seven typical samples

(1) $x = 0$ ($\bullet$), (2) $x = 0.025$ ($\triangle$), (3) $x = 0.05$ ($\blacktriangle$), (4) x = 0.1 ($\odot$), (5) x = 0.15 ($\blacksquare$), (6) x = 0.3 ($\square$), and (7) x = 0.5 ($\bigcirc$)

Figure 3. Variation of optical gap, E_g, with composition parameter, x.

Figure 4. Plot of ln $(\alpha h\nu)$ versus ln $(h\nu\text{-}E_g)$ for seven typical samples
(1) $x = 0$ (●), (2) $x = 0.025$ (▲), (3) $x = 0.05$ (△), (4) $x = 0.1$ (⊙), (5) $x = 0.15$ (■), (6) $x = 0.3$ (□), and
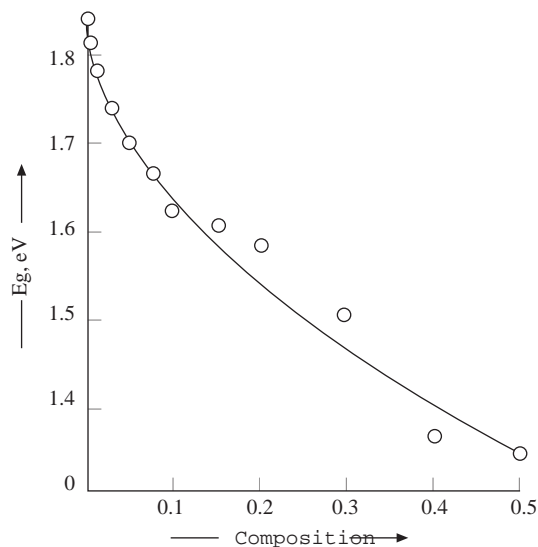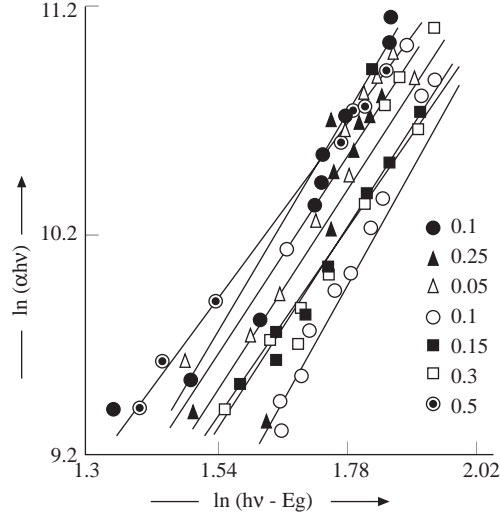(7) $x = 0.5$ (○)

3.4. Transport properties

The electrical conductivities of all these as-deposited structures were measured in the 300 K to 600 K temperature range and their temperature dependence can be fitted to an usual Arrheneous relation as

$$\sigma = \sigma_0 \exp(-E_{a\sigma}/KT), \tag{1}$$

where $E_{a\sigma}$ is the activation energy of an electrical conduction process and other terms have their usual significance. The plots of log σ vs inverse absolute temperature for these films were evaluated to determine the mode of conduction mechanism and the electron activation energies in the high and low temperature regions. It has been seen for the all the compositions that the conductivity increased with temperature and the activation energies in both low and high temperature regions are computed. The conductivity activation energy in the intrinsic conduction region varied from 0.792 to 0.864 eV as x was varied from 0 to 0.5. Whereas, it varied from 0.264 to 0.251 eV for the same change of Mn content in the samples for extrinsic conduction. In both these cases variations are similar and magnitudes of activation energies decreased initially , attain minimum at $x = 0.1$ and increased again for higher contents on Mn in CdSe. Figure 5 shows conductivity as a function of film composition, x at temperatures 298 K and 398 K. As one can readily see, conductivity increased with Mn^{2+} concentration up to $x = 0.1$, after which it decreased with further addition of Mn^{2+} in CdSe. The initial increase in the electrical conductivity is obviously due to the decrease in the band gap and enhanced grain structure of the material whereas the decrease in conductivity after $x = 0.1$ can be due to the increased disorder caused by the addition of increasing amount of Mn^{2+}, which caused the carrier mobility μ to decrease. The variation of electrical conductivity with temperature shows two distinct conduction regions corresponding to two activation energies and conduction mechanisms. Evaluation of these conduction mechanisms in two different regions is therefore of importance. Figure 6 shows an analysis wherein the high temperature region is characterized by a grain boundary-limited conduction mechanism, and hopping conduction mechanism is a characteristic of conduction in the low temperature zone [8, 10, 12].
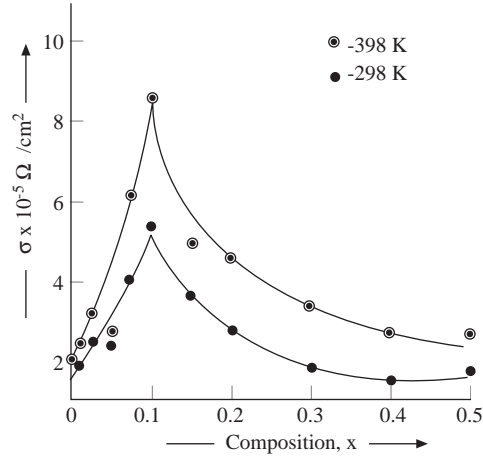
Figure 5. Variation of conductivity with composition parameter, x.
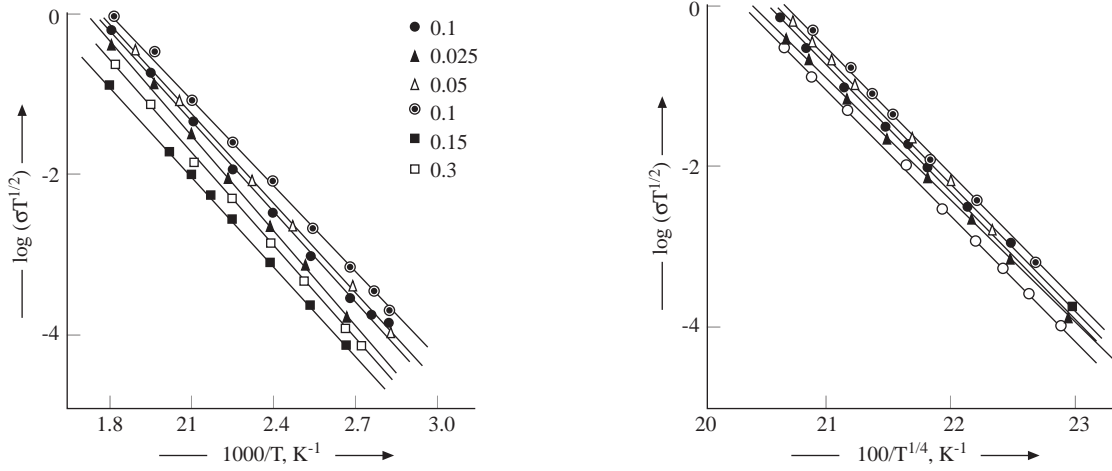

Figure 6a. Variation of log $(\sigma T^{1/2})$ versus $1000/T$ for six typical samples.
(1) $x = 0$ (●), (2) $x = 0.025$ (▲), (3) $x = 0.05$ (Δ),
(4) $x = 0.1$ (⊙), (5) $x = 0.15$ (■) and (6) $x = 0.3$ (□)

Figure 6b. Variation of log $(\sigma T^{1/2})$ versus $100/T^{1/4}$ for five typical samples.
(1) $x = 0$ (●), (2) $x = 0.025$ (▲), (3) $x = 0.05$ (Δ),
(4) $x = 0.1$ (⊙) and (7) $x = 0.5$ (◯)

The thermo-emf character of the samples was measured by establishing a temperature gradient and measuring the resulting voltage across the ends of each sample. The thermally generated voltage was measured in the temperature range 300 K to 450 K. The thermoelectric voltage was found to be negative in all samples, indicating n-type conduction in the samples. It is also observed that the temperature variation of thermo power is approximately linear at low temperature, but exhibits non-linear behavior at higher temperatures, obeying the power law dependence of temperature. This suggests that the material is of non-degenerate type and, for such semiconductors the thermo power is week. The thermal power can be expressed as

$$P = -K/e[(r + 5/2) + \ln(2\{2\Pi m_d^* KT)^{3/2}/nh^3\})], \tag{2}$$

where, A= $r+5/2$ is a thermoelectric factor that depends on the various scattering mechanisms, m_d^* is the density of states effective mass, n is the carrier density, and other parameters have their usual physical significance. The thermopower P and carrier concentration n are related as [11]

$$P = \pm 200(19.4 - \log n) \tag{3}$$

Figure 7 is a plot of the carrier density n and mobility μ as a function of the composition parameter x. It is seen that the carrier density and mobility varies with the film composition and temperature; the variation in carrier mobility is significant compared to the carrier concentration. This is suggestive of the scattering mechanism associated with the inter crystalline barrier potential [12]. The intercrystalline barrier potentials V_ϕ were therefore calculated for all the compositions and its composition dependence is shown in Figure 8.
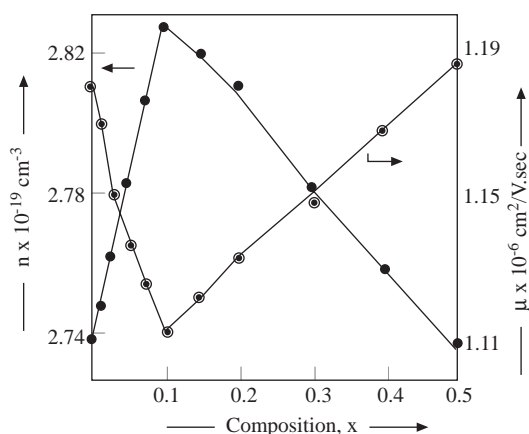

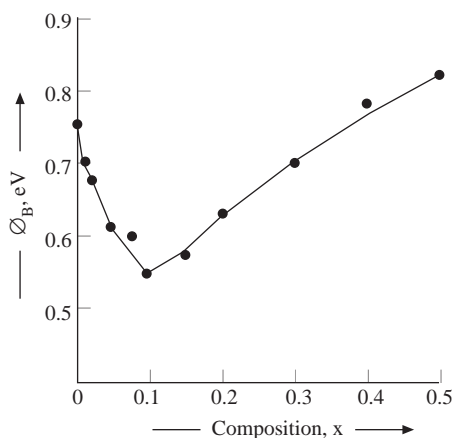**Figure 7.** Dependence of carrier density, n, and mobility, μ, on composition parameter, x.

Figure 8. Variation of barrier potential with composition parameter, x.

4. Conclusions

The synthesis of $Cd_{1-x}Mn_xSe(0 \le x \le 0.5)$ composite diluted semimagnetic semiconductor thin films is made feasible using a simple chemical growth process. The preparation parameters such as deposition temperature, time, pH, concentration of the basic materials and speed of the mechanical churning etc. were optimized to obtain good quality material. The samples were further characterized through some of the properties such as the materials composition, its crystallography, electrical conductivity, optical absorption, thermo power measurements etc to determine the materials characteristics, viz. mechanism of the conduction process, type of conduction, carrier density, mobility, optical band gap, type of transition etc., and their composition and temperature dependence.

References

[1] S. Mackowski, Nguyen The Khoi, A.Golnik, *Solid State Comm.,***107,** (1998), 67.

[2] T. Dietl, Handbook of semiconductors (Edited by T.S. Moss and S. Mohan), 1521 (1997).

[3] J. Kossut, and W. Dobrowolski, Chapman and Hall, London, 401 (1997).

[4] K. Shinji, Y. Tevai, K. Takita, T. Takamasu, G. Kido, N. Hsegwua, T. Kuroda and F. Minami, *Journal of Crystal Growth,* **215,** (2000),149.

[5] K.L. Chopra and S.R. Das, Thin film solar cells (Plenum press, New York), (1983).

[6] V.S. Karande, S.H. Mane, V.B. Pujari and L.P. Deshmukh, Indo-Japan Symposium On Advances In Electronic Materials, November 06, 2002 (High Rank Oral Presentation)

[7] C.V. Suryanarayanan, A.S. Kakhamanan, V. Subramanan and R.K. Kumar, *Bull. Electrochem,* **2,** (1986), 57.

[8] E.U. Masumdar , V.B. Gaikwad , V.B. Pujari and L.P. Deshmukh , *J.Mat. Sci.; J. Mat. Elect.* **14,** (2003), 43.

[9] D. Bhattacharya, S. Chaudhuri and A.K. Pal, *Vacuum,* **43**, (1992), 313.

[10] V.B. Patil, D.S. Sutrave, G.S. Shahane and L.P. Deshmukh, *Indian Journal of Pure and Applied Physics,* **39**, (2001), 184.

[11] J. George, T.I. Palson and K.S. Joseph, *Solid state comm.,* **58,** (1986), 605.

[12] R.L. Petriz, *Phys. Rev,* **104,** (1956), 1508.